

Iron-bearing phases affecting the colour of upper Neogene clayey sediments from Dymaczewo Stare, west-central Poland

Jakub Klęsk^{1*}, Artur Błachowski², Ryszard Diduszko³, Łukasz Kruszewski⁴,
Marek Widera¹

¹ Institute of Geology, Adam Mickiewicz University, Krygowskiego 12, 61-680 Poznań, Poland;
e-mails: jnklesk@gmail.com, widera@amu.edu.pl

² Faculty of Geology, Geophysics and Environmental Protection, AGH University of Science and Technology,
al. Mickiewicza 30, 30-059 Kraków, Poland; e-mail: sfbalcho@cyf-kr.edu.pl

³ Institute of Microelectronics and Photonics, Łukasiewicz Research Network, Wólczyńska 133, 01-919 Warszawa,
Poland; e-mail: diduszko@ifpan.edu.pl

⁴ Institute of Geological Sciences, Polish Academy of Sciences, Twarda 51/55, 00-818 Warszawa, Poland;
e-mail: lkruszewski@twarda.pan.pl

*corresponding author, e-mail: jnklesk@gmail.com

Abstract

The present paper investigates the colour dependence of mineral compositions in clay-rich sedimentary strata, mainly clayey silts, the emphasis being on iron-bearing minerals (rather than clay minerals) by using powder X-ray diffraction (PXRD) and ⁵⁷Fe Mössbauer spectroscopy (⁵⁷Fe-MS). The PXRD-based phase analysis has demonstrated the variable compositions of samples, consisting of, *inter alia*, quartz, calcite or gypsum, and admixtures of potassium feldspars and plagioclase. Hematite + goethite (sample D1, dark red), goethite (sample D2, pinkish brown), poorly crystalline goethite (sample D3, orange) and jarosite (sample D4, yellow) have been distinguished. A very low jarosite content was detected in sample D5 (light grey); this did not affect its colour. The potential yellow/brown shades in sample D6 (dark grey), coming from trace amounts of jarosite, are masked by macroscopically visible organic matter. In the case of the two last-named samples (D5 and D6), with trace amounts of Fe-bearing minerals, it is most likely that the organic matter was effective in influencing the light and dark grey colour of the sediment, respectively.

Key words: mineral composition, powder X-ray diffraction (PXRD), iron minerals, ⁵⁷Fe Mössbauer spectroscopy (⁵⁷Fe-MS), 'Poznań Clays', Mio-Pliocene

1. Introduction

Vari-coloured sediments and rocks have been the subject of human interest for at least several millennia. This interest arose mainly from the fact that they were the source of pigments that were used for colouring various products (e.g., paints, artistic works, ceramics, glass, etc.) and for the production

of building materials such as bricks, tiles, etc. (e.g., Valanciene et al., 2010; Habashi, 2016). Over the last century, the colour of sedimentary rocks has been recognised as an important indicator of their origin, weathering and diagenesis; this has been summarised by, among others, McBride (1974), Myrow (1990) and Tucker (2011).

The Neogene clay-rich strata examined here have been excavated in west-central Poland for the production of red bricks since at least the 16th century (Maciaszek et al., 2020). The colour of these sediments, predominantly classified as clayey silts, has been subjectively specified in all geological documentation and scientific papers. Of course, the main pigments such as Fe-bearing hematite, goethite and jarosite, distinguished and discussed in the present study, were already known from numerous studies of the mineralogy of these levels at various localities in the Polish Lowlands (e.g., Dyjor et al., 1968; Wyrwicki & Wiewióra, 1981; Wagner, 1982; Choma-Moryl, 1988; Górniak et al., 2001; Bojakowska et al., 2010; Duczmal-Czernikiewicz, 2010, 2013; and references therein). However, the main purpose of those studies was not sediment colour, unlike the present paper. It can even be said that, until now, it was believed that their colour was solely due to their organic matter contents – grey, as well as depended on variable oxidation states (Fe^{3+} and Fe^{2+}) – red, flamy, green and blue (Piwocki et al., 2004).

Much emphasis has been placed on the mineral composition of the ‘Poznań Clays’, especially in the fraction smaller than 2 μm (Wiewióra & Wyrwicki, 1976; Wyrwicki & Maliszewska, 1977), and its chemical composition (Wichrowski, 1981). It has been repeatedly postulated in Polish literature that one of the main factors in the formation of the clay-rich sediments examined here were soil processes that had an impact on their mineral composition (Różycki, 1972; Górniak et al., 2001; Piwocki et al., 2004; Widera, 2007; Duczmal-Czernikiewicz, 2010, 2013; Maciaszek et al., 2020; and references therein). Thus, their mineral composition was shown to include (in variable proportions) quartz, beidellite, kaolinite, illite, feldspar, chlorite and iron oxides/oxyhydroxides such as, for example, hematite and goethite (Wiewióra & Wyrwicki, 1976; Wichrowski, 1981). The chemical composition is dependent mainly of the mineral composition (Wichrowski, 1981) and reflects the process of chemical weathering that occurred both during and after sedimentation of the deposits studied (Duczmal-Czernikiewicz, 2010).

The main goal of the present paper is to verify the above-mentioned hypothesis of Piwocki et al. (2004) that the colour of the ‘Poznań Clays’ depended generally on organic matter and the content of iron (Fe^{3+} , Fe^{2+}) oxides and hydroxides. This will be achieved by answering the question of whether only those components listed by Piwocki et al. (2004) affected the colour of the sediment, or not. Therefore, we have determined the mineral composition of chosen samples of different colours and specified the iron oxidation states in iron-containing minerals.

2. Geological outline

2.1. Lithostratigraphy of the upper Neogene

The fine-grained deposits studied here are assigned to the Wielkopolska Member, which is the upper unit of the Poznań Formation. This formation is the youngest Neogene unit in the area; it covers almost a quarter (~75,000 km²) of the territory of Poland (Areń, 1964; Piwocki et al., 2004). In fact, these levels include only the uppermost strata of the Wielkopolska Member, namely the ‘flamy clays’ (Ciuk, 1970; Dyjor, 1970). Together with the underlying ‘green clays’, these constitute the Wielkopolska Member (Piwocki & Ziemińska-Tworzydło, 1997).

The Wielkopolska Member overlies the Grey Clays Member, with the 1st Mid-Polish Lignite Seam and the ‘grey clays’ at the top (see Piwocki & Ziemińska-Tworzydło, 1997, fig. 1; Widera, 2013, fig. 2), and is itself overlain by Quaternary glaciogenic deposits. The time of deposition of the Wielkopolska Member has been determined as late middle Miocene to earliest Pliocene (Piwocki & Ziemińska-Tworzydło, 1997; Troć & Sadowska, 2006; Kędzior et al., 2021; Widera et al., 2021).

2.2. Origin of the Wielkopolska Member

For less than two decades it was assumed that the clay-rich sediments of the Wielkopolska Member were of fluvial origin (Badura & Przybylski, 2004; Piwocki et al., 2004). Previously, for a century (between the mid-1900s and mid-2000s) the clay-rich deposits, which constitute the dominant part of the originally called ‘Poznań Clays’, were attributed mainly to a ‘Pliocene lake’ (e.g., Areń, 1964). Later, between 1960 and 1970, it was suggested that the lacustrine basin (lake) was occasionally influenced by marine incursions from the Carpathian Foredeep area (e.g., Dyjor et al., 1968; Dyjor, 1970).

In fact, the levels of the Wielkopolska Member studied accumulated in the overbank zone of a late Neogene river system. This is confirmed, among others, by the presence of numerous sandy and sandy-muddy bodies that represent river palaeochannels, surrounded by the above-mentioned vari-coloured clayey silts. Based on sedimentological studies it has been concluded that these strata formed in an environment of a late Neogene anastomosing (Widera, 2013; Widera et al., 2017, 2019; Maciaszek et al., 2020) or anastomosing to meandering river system (Zieliński & Widera, 2020; Kędzior et al., 2021).

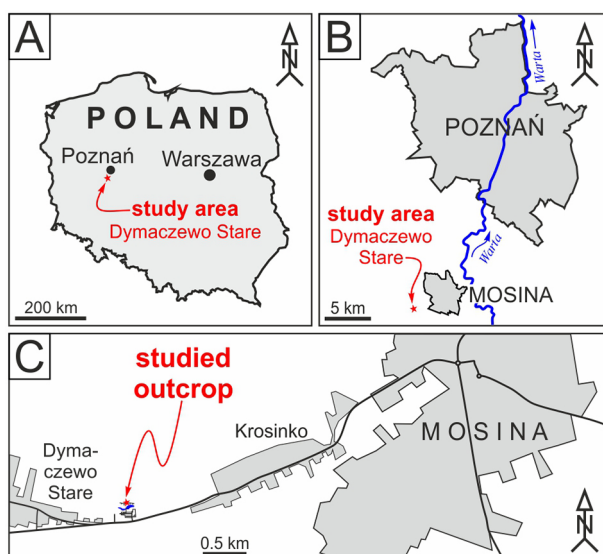


Fig. 1. Locality map of Dymaczewo Stare. **A, B** – Study area in the background of Poland and Poznań, respectively; **C** – Detailed location of the outcrop studied (co-ordinates 52°13'49.8"N, 16°47'28.7"E).

The terrestrial/fluviol origin of the Wielkopolska Member is additionally supported by mineralogical and geochemical studies, which have been conducted in various parts of the sedimentary basin (e.g., Wyrwicki & Wiewióra, 1981; Wagner, 1982;

Choma-Moryl, 1988; Górniak et al., 2001; Duczmal-Czernikiewicz, 2010, 2013). Among other sites, Duczmal-Czernikiewicz (2010, 2013) conducted her research at the Dymaczewo Stare outcrop (Fig. 1), the same exposure which we have examined for the present study. She focused mainly on clay mineralogy and determined that pedogenetic processes had affected these sediments.

3. Material and methods

3.1. Field data and sampling

In the spring of 2021, fieldwork was carried out at the Dymaczewo Stare outcrop, which is located in west-central Poland, ~15 km south of the city of Poznań and <3 km west of the town of Mosina (Fig. 1). This outcrop is a former pit in which the 'Poznań Clays' were excavated for the production of red bricks until 1994. Thus, the quarry face of clays (up to 4 m in height and >15 m in length) has been exposed for at least 35 years (Fig. 2A).

During the fieldwork, macroscopic observations, descriptions and photographic documentation of sediments were carried out first. Subse-

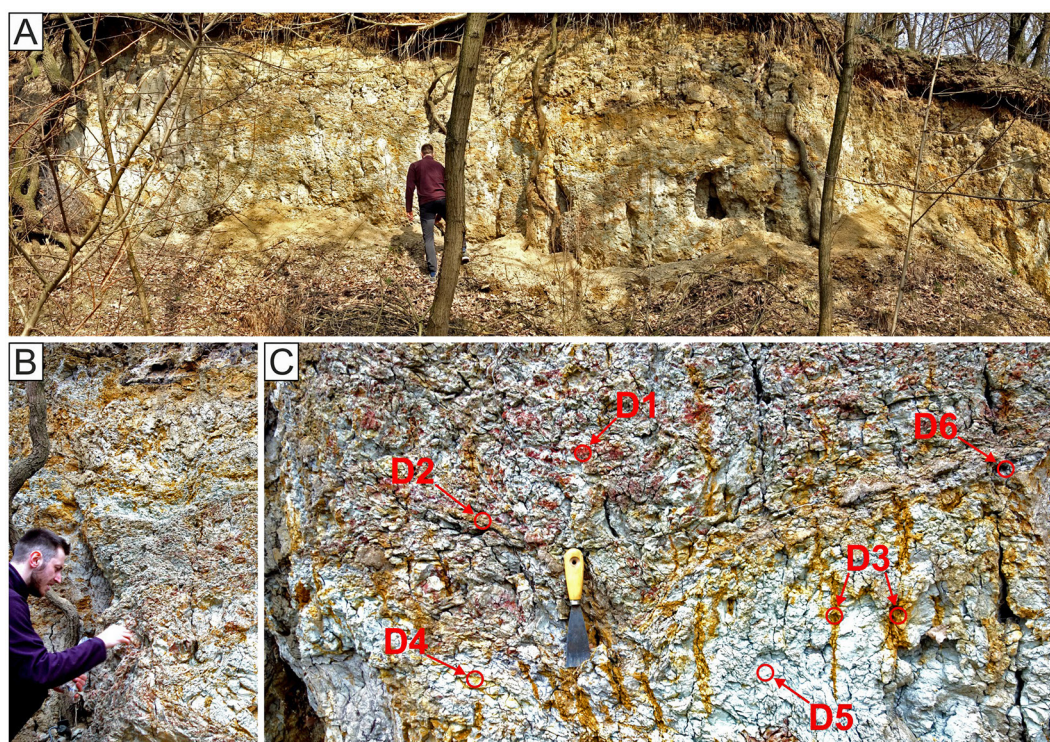


Fig. 2. Vari-coloured 'Poznań Clays' at Dymaczewo Stare. **A** – Broad north view of the outcrop section, with the first author (JK, 1.93 m tall) as scale; **B** – Clear zonation of colours in the vertical section of strata; **C** – Close-up, showing different colours of the clayey silts; note the vertical orange strings and sampling sites D1–D6.

quently, six samples, of clearly different colours (Fig. 2B, C), were collected for further analyses in the laboratory.

3.2. Colour determination

The colours described in the field and laboratory differ from those shown in the illustrations (e.g., in graphical and PDF files) or in the printed version of scientific papers. Thus, on account of subjective perceptions of colours, we have here additionally included a description of colours of samples measured on the basis of the RGB (Red–Green–Blue) values (Fig. 3). The CorelDRAW X8 computer program was used to digitise sediment colours.

3.3. Powder X-ray diffraction (PXRD)

A Rigaku SmartLab 3kW diffractometer, located at the Łukasiewicz Research Network – Institute of Microelectronics and Photonics (Warsaw), was used for powder X-ray diffraction analysis under the following conditions: Bragg-Brentano geometry, filtered $\text{CuK}\alpha$ radiation, $5\text{--}90^\circ$ 2θ range, 0.02° 2θ step, and a linear position-sensitive detector. The results were evaluated using the EVA software of Bruker.

The samples were prepared in the way described by Kruszewski (2013) and Mederski et al.

(2021). They were ground in a mortar into a powder, in portions of 1–2 g (depending on sample density). Subsequently, samples were placed in standard perforated cuvettes (to minimise the phenomenon of preferential orientation) and irradiated in the diffractometer. The preparation typical of clay-rich sediments, i.e., Johnson's method, was not used, because the aim of the present work was to characterise mineral pigments, rather than study clay minerals.

3.4. ^{57}Fe Mössbauer spectroscopy (^{57}Fe -MS)

The ^{57}Fe -MS measurements were performed at room temperatures in transmission geometry applying the RENON MsAa-4 spectrometer (Górnicki et al., 2007; Błachowski et al., 2008), which operates in the round-corner triangular mode and is equipped with the LND Kr-filled proportional detector. A He-Ne laser-based interferometer was applied to calibrate a velocity scale. A commercial $^{57}\text{Co}(\text{Rh})$ source, made by RITVERC GmbH, was used. The source line-width $\Gamma_s = 0.106(5)$ mm/s was derived from the fit of the Mössbauer spectrum of a $10\mu\text{m}$ -thick $\alpha\text{-Fe}$ foil. The transmission integral approximation was applied to fit the Mössbauer spectra using the MOSGRAF data processing software suite. All line widths reported stand for the absorber line width Γ_a within the transmission integral. Referring to the Lorentzian-shaped spectral peak line

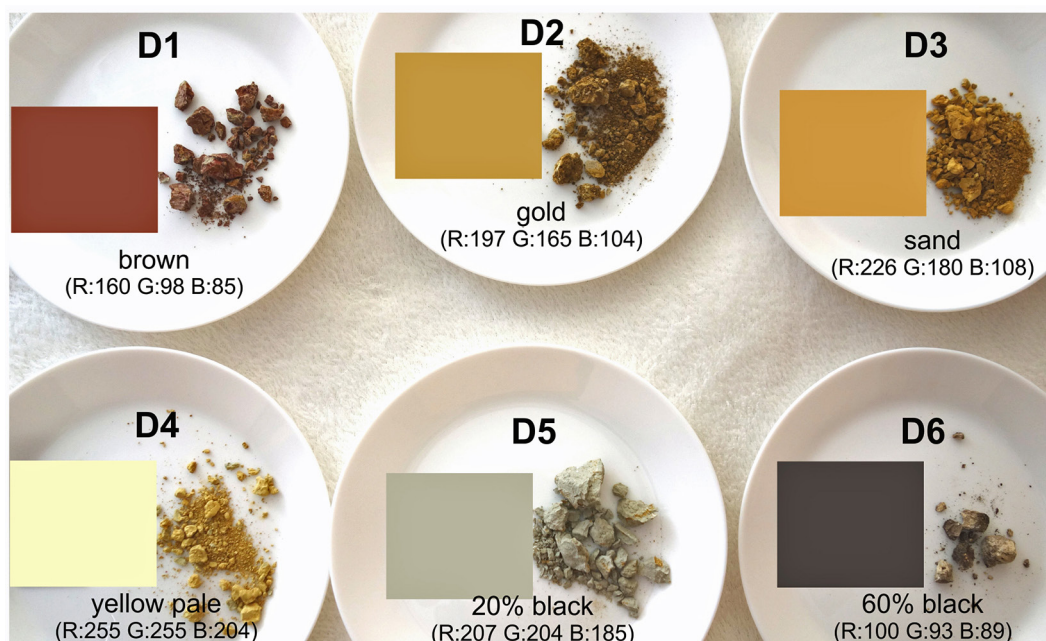


Fig. 3. The colour names of the samples identified in the computer RGB system. Note the RGB values (ranging from 0 to 255) in 24-bit colour system; D1–D6 correspond to sample numbers.

width with FWHM (full width at half maximum), it may be assumed, with some approximation, that $\text{FWHM} = \Gamma_a + \Gamma_s$. The spectral isomer (centre) shifts IS are reported with respect to the isomer (centre) shift of room temperature α -Fe. The absorbers for Mössbauer measurements were prepared using 40 mg/cm² of the samples studied, as previously described by Górnicki et al. (2007) and Błachowski et al. (2008).

⁵⁷Fe-MS hyperfine parameters were used to identify Fe-bearing minerals. The values of the isomer shift, quadrupole splitting and hyperfine magnetic field were compared with standard literature values (Dyar et al., 2006; Murad, 2010), which allowed for the assignment of a given spectrum component to a specific mineral or group of minerals. Some of the minerals have been identified as nanomaterials with an estimated particle size below *c.* 10 nm (Murad, 2010). Mössbauer spectra of these minerals are characterised by a significant broadening of the line width Γ_a , which is caused by the superparamagnetic relaxation of electron spins in a magnetic domain of nanoparticles. The phenomenon of superparamagnetism depends on particle size (crystallinity) and is a function of temperature. The limit size of nanocrystals below which superparamagnetism manifests at room temperature is about 10 nm (Murad, 2010).

4. Results

4.1. Field and laboratory observations of sediment colour

The clayey silts studied do not occur in their primary sedimentary position because they are clearly glaciotectonically disturbed. Their motley colours are their most distinctive feature. At the Dymaczewo Stare outcrop, sediment colour does not show any zonal order (Fig. 2A, B), with exception of vertical orange strings, which are most likely associated with infiltrating water and precipitation of iron minerals in the fractures and on surfaces exposed (Fig. 2C).

In the field, the colours of samples (D1–D6) taken for further study was defined as follows: cherry (dark-red) – D1, pinkish brown – D2, orange – D3, yellow – D4, light grey – D5 and dark grey – D6 (Fig. 2). In the laboratory, however, the colour names of the same samples, digitised by computer in the RGB system, differed from those listed above. The following colours correspond to these: brown – D1,

gold – D2, sand – D3, pale yellow – D4, 20% black – D5, and 60% black – D6, respectively (compare Figs. 2, 3). In order not to create additional terminological confusion, the colours that have been macroscopically determined in the field are used consistently throughout the remainder of the present paper.

4.2. Mineral composition of bulk samples

Sample D1.

The cherry (dark-red) sample D1 has quartz, hematite and goethite as major minerals, with smaller amounts of microcline, illite, kaolinite, smectite and orthoclase. Muscovite cannot be ruled out in this dark-red sample (Fig. 4; Table 1).

Sample D2.

The pinkish brown sample D2 comprises mainly quartz, with calcite as an additional major component. The calcite is magnesian, as suggested by the position of its main reflection ($d = 3.026\text{\AA}$). Another important, albeit minor, constituent is plagioclase, best-fittable to albite. Minor minerals include K-feldspar (microcline, orthoclase), muscovite, illite, kaolinite, smectite and goethite (Fig. 4; Table 1).

Sample D3.

The orange sample D3 contains quartz and calcite as major minerals, with calcite most likely slightly prevailing over quartz. It also contains small amounts of plagioclase, K-feldspar (microcline, orthoclase), goethite, kaolinite, illite and smectite (Fig. 4; Table 1).

Sample D4.

The yellow sample D4 stands out because jarosite is its major component (Fig. 4). The second most important constituent is quartz, with traces of gypsum, kaolinite, illite, smectite and, possibly, orthoclase (Fig. 4; Table 1).

Sample D5.

The light grey sample D5 is quartz rich. Its subordinate components are gypsum, and minor amounts of jarosite, illite, kaolinite and smectite. In addition, trace amounts of anatase (titanium dioxide, tetragonal) are seen in this sample. A weak reflection at 3.40 probably represents aragonite (Fig. 4; Table 1).

Sample D6.

The dark grey sample D6 is also quartz rich, and also contains gypsum. Illite, kaolinite, smectite,

4.3. Oxidation state of iron atoms

The results of Mössbauer spectroscopy (^{57}Fe -MS), relating to iron atoms, are presented in Figure 5 and Table 2. Thus, in the case of sample D1, iron atoms are mainly in hematite in a bulk-crystallised form (36% – percentage of Fe atoms in the sample) and a nano-crystallised form (36%) [see Section 3.4 for terminological explanation]. In sample D2, iron atoms are present in goethite in a bulk-crystallised form (22%) and a nano-crystallised form (59%) (22%) and a nano-crystallised form (59%).

Surprisingly, in sample D3, iron atoms are in a mixture of goethite, mainly in the form of nanocrystals (45%), and jarosite (21%). This result is somewhat incompatible with the PXRD analysis due to non-homogeneity of the material under study and simultaneous ^{57}Fe -MS and PXRD measurements of

two subsamples D3 extracted from it (compare Figs. 2C, 4, 5).

In sample D4, iron atoms occur in jarosite, and it is this mineral that definitely determines the yellow colour of the sample. The last two samples studied (D5 and D6) contain negligible amounts of iron, possibly in silicates (Fig. 5; Table 2). Due to the very small amounts of iron in these samples, the ^{57}Fe -MS method does not allow to determine definitively in which silicates Fe is present.

Based on ^{57}Fe -MS data, it may be concluded that in the material studied, iron atoms are present almost exclusively in the state of trivalent ions (Fe^{3+}). On the other hand, between samples of different colours, there is significant variation in the composition of iron-bearing minerals and their crystalline form (Fig. 5; Table 2).

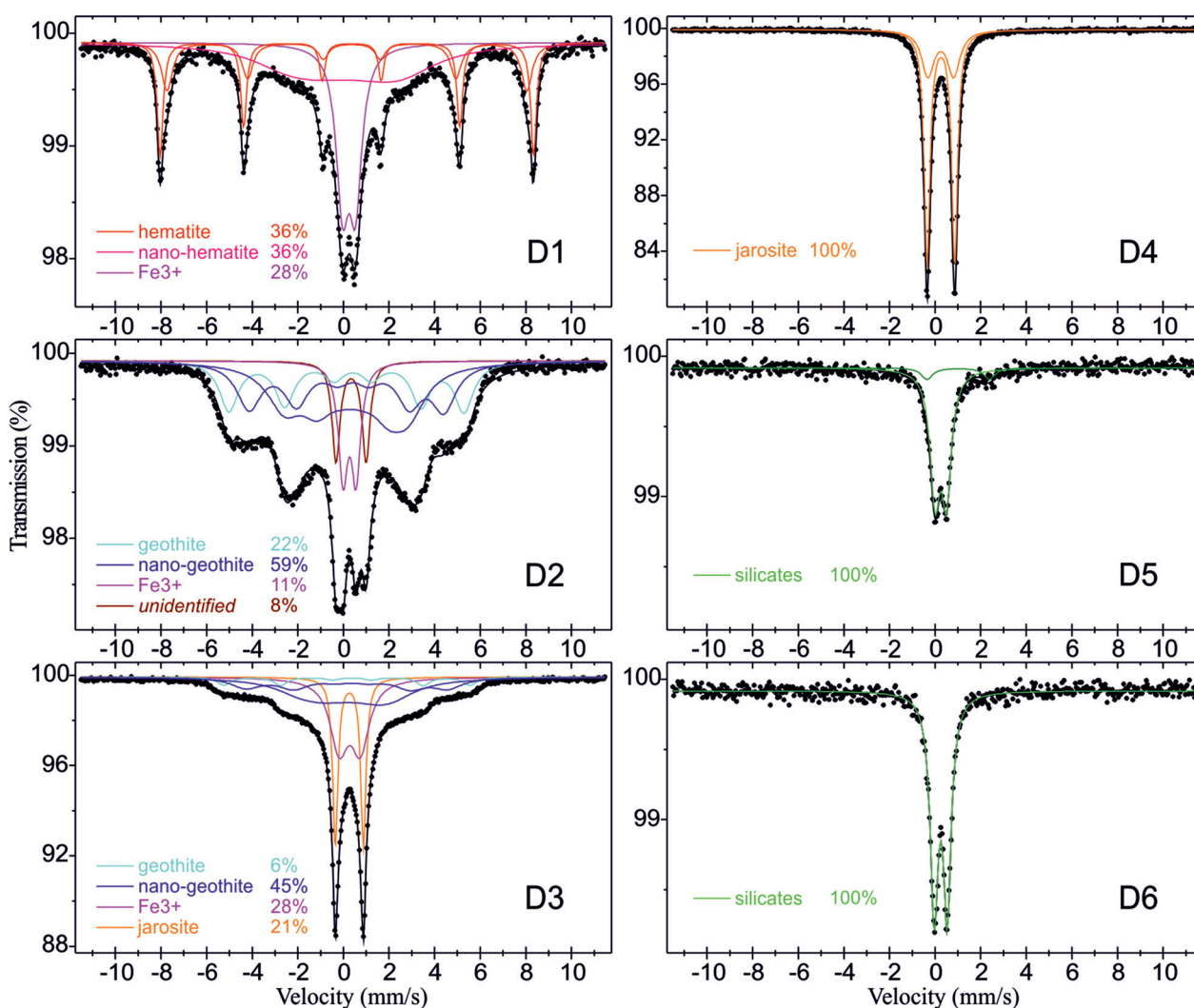


Fig. 5. ^{57}Fe Mössbauer spectra of the Dymaczewo Stare samples. The percentages shown correspond to the relative distribution of Fe atoms into respective iron-bearing minerals. The sample numbers are the same as in Figures 3 and 4, but due to the non-homogeneity of the material under study, the PXRD and ^{57}Fe -MS results obtained may not be identical and should be treated only for comparative purposes. See Table 2 for more details of spectral components.

Table 2. Hyperfine parameters for ^{57}Fe Mössbauer spectra shown in Figure 5. Symbols stand for: A (%) – area of the spectral component corresponding to the relative distribution of Fe atoms into respective iron-bearing minerals; IS – isomer (centre) shift relative to room temperature $\alpha\text{-Fe}$; QS – quadrupole splitting; Γ_a – absorber line width (within transmission integral approximation); B – hyperfine magnetic field. Errors are in the order of unity for the last digit shown or are shown in brackets. The colours of the samples are related to Figure 3. The spectral component marked as Fe^{3+} may correspond to nano-(Fe-oxide or hydroxide). (*) For samples D5 and D6 with traces of Fe-bearing minerals, the spectrum is assigned to silicates and their distinction using the MS method is uncertain (Hawthorne, 1988; Murad & Cashin, 2004; Stevens et al., 2005; Dyar et al., 2006; Murad, 2010). Sample numbers as in Figure 3.

Sample (colour)	Fe-bearing mineral/Fe-valence	A (%)	IS (mm/s)	QS (mm/s)	Γ_a (mm/s)	B (Tesla)
D1 (cherry, dark-red/brown)	hematite	20(2)			0.21	50.8
		16(2)	0.37	-0.21	0.45	48.9
	nano-hematite	36(3)			3.7	16
	Fe^{3+}	28(1)	0.36	0.57	0.56	-
D2 (pink-brown/gold)	goethite	22(2)			0.9	32.0
	nano-goethite	26(3)	0.38	-0.28	1.2	26.5
		33(4)			1.7	17
	Fe^{3+}	11(1)	0.38	0.57	0.39	-
	<i>unidentified</i>	8(1)	0.45	1.31	0.31	-
D3 (orange/sand)	goethite	6(1)			0.60	33.5
	nano-goethite	16(3)	0.37	-0.22	1.5	27
		29(5)			2.5	13
	Fe^{3+}	28(3)	0.39	0.93	0.84	-
	jarosite	21(1)	0.37	1.23	0.17	-
D4 (yellow/pale yellow)	jarosite	73(3)	0.37	1.21	0.18	-
		27(4)	0.37	1.13	0.54	-
D5 (light grey/20% black)	silicate*	90(3)	0.36	0.50	0.41	-
		10(2)	1.1	2.7	0.5	-
D6 (dark grey/60% black)	silicate*	100	0.36	0.57	0.32	-

5. Interpretation and discussion

The 'Poznań Clays' in the Polish Lowlands have been examined mineralogically in detail many times, both at the Dymaczewo Stare outcrop (Duczmal-Czernikiewicz, 2010, 2013), as in other parts of the sedimentary basin (e.g., Wiewióra & Wyrwicky, 1976; Wyrwicky & Maliszewska, 1977; Wichrowski, 1981; Wyrwicky & Wiewióra, 1981; Wagner, 1982; Choma-Moryl, 1988; Górniak et al., 2001; Wiedera, 2007; Bojakowska et al., 2010). All studies have shown that smectite and illite-smectite are the dominant phases among clay minerals in all colour varieties of the sediments studied. Within the context of the present research, this statement was best documented by Górniak et al. (2001, fig. 2), who proved a similar composition of minerals in the clay fraction for samples of the 'Poznań Clays' of different colour.

The fine-grained and vari-coloured sediments at Dymaczewo Stare examined are strongly disturbed glaciotectionally, creating the axial zone of terminal moraine. They were uplifted to the present land level during the Pleistocene, facilitating both their

exploitation and weathering. Thus, the currently observed colour of these sediments is a result of their original Neogene colour, plus overlapping mineral transformations, including contemporary soil processes and oxidation by external factors such as air, water, micro-organisms, etc. (see Fig. 2). In consideration of this, it is impossible to determine when exactly the currently observed colour of the strata studied was formed.

Following PXRD and ^{57}Fe -MS, the 'warmest' colours (cherry and pinkish brown) in our samples result from relatively high contents of hematite or goethite in samples D1 and D2, respectively. The yellow colour is caused by the presence of jarosite (sample D4), while a mixture of jarosite with a small amount of goethite renders the sediment orange (sample D3). In the case of sample D3 of the same colour, but tested in PXRD, the orange colour derives from the presence of goethite, rather than jarosite, which was found using the ^{57}Fe -MS (compare Figs. 4, 5). Finally, light grey and dark grey colours (samples D5 and D6) indicate the very low contents of iron in the sediments studied, with in both cases, a negligible quantity of iron cations in

silicates present (Fig. 5; Table 2). In such a case, other researchers would not exclude the presence of organic matter in the sediment (e.g., McBride, 1974; Myrow, 1990). This is evidently confirmed in the case of sample D6, in which the organic matter (tiny roots) is macroscopically visible.

PXRD and ^{57}Fe -MS analyses show beyond doubt that hematite imparts a cherry (dark red) colour to sample D1. Any yellow, brown or intermediate colour coming from goethite is here masked by hematite. Samples D2 and D3 bear the comparatively smallest amounts of minerals (goethite) as potential pigments. The pinkish and brownish hue of these samples results from trace goethite, both bulk- and nano-crystallised, as confirmed by ^{57}Fe -MS (see Fig. 5). A probably poorly crystalline goethite was the sole colourant detected in samples D2 and D3. Due to the low-crystalline nature of the goethite, one may also expect the presence of amorphous Fe oxyhydroxides in this and other goethite-bearing samples studied (Tobia et al., 2014; Laureijs et al., 2021). On the other hand, the presence of jarosite in sample D3 is most likely due to the fact that the D3 subsamples, studied using ^{57}Fe -MS and PXRD, differed mineralogically, although they had the same colour, i.e., orange (see Fig. 2C).

Both research methods used (PXRD, ^{57}Fe -MS) have confirmed that the yellow colour of sample D4 stems exclusively from jarosite (compare Figs. 4, 5). The iron-rich members of the alunite supergroup are typically yellow or orange-yellow and brownish yellow (Anthony et al., 2003). Samples D5 and D6 (see Fig. 4), which are light grey and dark grey, bear only trace jarosite. Such insignificant amounts of jarosite are too low to impart a yellow/brown colouration. To sum up, the sediments studied contain almost exclusively Fe^{3+} in such colouring minerals (pigments) as hematite, goethite and jarosite (compare Figs. 4, 5). This can be explained by the fact that the clayey silts at Dymaczewo Stare had been exposed to post-depositional oxidising agents for a long time (see Fig. 2).

Finally, the role of organic matter in colouring of sedimentary rocks needs to be briefly discussed here. The total amount of organic matter in the sediment may determine its colour. Based on empirical data supplied by Myrow (1990), it may be concluded that even small amounts of organics (0–0.3 wt.%) can give the sediment a grey shade. In turn, >0.3 wt.% of organic matter already shields other colours, giving the sediment a grey to black colour (Myrow, 1990). This is most likely the case for sample D5 and certainly (visible plant roots) for sample D6.

6. Conclusions

X-ray diffraction (PXRD) has allowed the mineral composition of the entire sediment sample to be determined, and additionally ^{57}Fe Mössbauer spectroscopy (^{57}Fe -MS) has provided the exact iron oxidation state in the minerals in which it was present. Thus, the results of the PXRD method show that quartz dominates in the multi-coloured samples studied. Other major minerals varied from sample to sample: goethite, hematite – sample D1; calcite (calcite<quartz) – sample D2; calcite (calcite>quartz) – sample D3; jarosite (jarosite>quartz) – sample D4; and gypsum (gypsum<quartz) – samples D5 and D6. Moreover, our analysis proves that hematite, goethite and jarosite have the greatest influence on colour in samples D1–D4. Traces of jarosite were also found in samples D5 and D6, but they have a grey shade which would be linked to the presence of organic matter, both in trace (sample D5) and significant (sample D6) amounts.

The colour of the clayey silts studied results from the occurrence of iron phases, as shown by the ^{57}Fe -MS method. In samples D1–D4, Fe^{3+} dominates, which is interpreted to have resulted from post-depositional oxidation. A more or less 'warm' colour is not influenced by the total content of Fe^{3+} cations, but by their presence in certain mineral phases, such as hematite, goethite and jarosite. It should be emphasised, however, that in addition to the pigments (colouring minerals) mentioned, the contents of organic matter also have an impact on the colour of clay-rich sediments. Samples D5 and D6, which contain very low amounts of iron-bearing minerals, are a good example.

Summing up, the colour of the clayey strata examined depends on the contents of organic matter and Fe oxides (e.g., hematite), which means that the hypothesis put forward by Piwocki et al. (2004) is verified. However, it may be influenced by Fe hydroxides and hydrous Fe oxides (e.g., goethite). Fe and K hydrous sulphates (e.g., jarosite) can also give a characteristic yellow colour to the sediments studied. The macroscopically defined orange colour may derive from the presence of both jarosite and goethite.

Acknowledgements

We wish to extend our thanks to the anonymous reviewers and the editor, J. Biernacka, for their critical comments, advice and editorial help, respectively, which improved the final version of the typescript. Mössbauer measurements were performed by one

of us, AB, using equipment of the Mössbauer Spectroscopy Laboratory at the Pedagogical University (Kraków, Poland). Finally, the current research was partially financed by the National Science Centre (Poland), grant no. 2017/27/B/ST10/00001.

References

- Anthony, J.W., Bideaux, R.A., Bladh, K.W. & Nichols, M.C. (eds.), 2003. Handbook of Mineralogy, Mineralogical Society of America, Chantilly, VA 20151-1110, USA. <http://www.handbookofmineralogy.org/pdfs/anatase.pdf>.
- Areń, B., 1964. Atlas geologiczny Polski. Zagadnienia stratygraficzno-facjalne. Trzeciorząd, 11/a [Geological atlas of Poland: stratigraphic and facies problems. Tertiary, 11/a]. Wydawnictwa Geologiczne, Warszawa.
- Badura, J. & Przybylski, B., 2004. Evolution of the Late Neogene and Eopleistocene fluvial system in the foreland of the Sudetes Mountains, SW Poland. *Annales Societatis Geologorum Poloniae* 74, 43–61.
- Błachowski, A., Ruebenbauer, K., Żukrowski, J. & Górnicki, R., 2008. Early design stage of the MsAa-4 Mössbauer spectrometer. *Acta Physica Polonica A* 114, 1707–1713.
- Bojakowska, I., Barański, P., Iwasińska-Budzyk, I. & Retka, J., 2010. Zróżnicowanie zawartości pierwiastków śladowych w ilach poznańskich [Variability of the content of trace elements in Poznań series clays]. *Górnictwo i Geologia* 5, 31–39.
- Choma-Moryl, K., 1988. Variability of physical properties of the Poznań Clays from the area of Wrocław, with reference to their genesis and lithostratigraphy. *Geologica Sudetica* 23, 1–63.
- Ciuk, E., 1970. Schematy litostratygraficzne trzeciorzędu Niżu Polskiego [Lithostratigraphic schemes of the Tertiary from the Polish Lowlands area]. *Kwartalnik Geologiczny* 14, 754–771.
- Duczmal-Czernikiewicz, A., 2010. *Geochemistry and mineralogy of the Poznań Formation (Polish Lowlands)*. Adam Mickiewicz University Press, Poznań, 88 pp.
- Duczmal-Czernikiewicz, A., 2013. Evidence of soils and palaeosols in the Poznań Formation (Neogene, Polish Lowlands). *Geological Quarterly* 57, 189–204.
- Dyar, M.D., Agresti, D.G., Schaefer, M.W., Grant, Ch.A. & Sklute, E.C., 2006. Mössbauer Spectroscopy of Earth and Planetary Materials. *The Annual Review of Earth and Planetary Science* 34: 83–125.
- Dyjur, S., 1970. Seria poznańska w Polsce zachodniej [The Poznań series in West Poland]. *Kwartalnik Geologiczny* 14, 819–835.
- Dyjur, S., Bogda, A. & Chodak, T., 1968. Preliminary studies on the mineral composition of the Poznań Clays. *Rocznik Polskiego Towarzystwa Geologicznego* 38, 491–510.
- Górniak, K., Szydłak, T., Sikora, W.S., Gawel, A., Bahranowski, K. & Ratajczak, T., 2001. Minerale ilaste w różnobarwnych odmianach skał występujących nad pokładem węgla brunatnego w rejonie Konina [Clay minerals in colourful rocks appearing over lignite deposits in Konin region]. *Górnictwo Odkrywkowe* 43, 129–139.
- Górnicki, R., Błachowski, A. & Ruebenbauer, K., 2007. Mössbauer Spectrometer MsAa-3. *Nukleonika* 52 (suppl. 1), S7–S12.
- Habashi, F., 2016. Pigments through the Ages. *International Ceramic Review* 65, 156–165.
- Hawthorne, F.C., 1988. Mössbauer spectroscopy. In: *Spectroscopic Methods in Mineralogy and Geology* (ed. F.C. Hawthorne): 18, 311–312. Reviews in Mineralogy, Mineralogical Society of America, Chantilly, Virginia.
- Kędzior, A., Widera, M. & Zieliński, T., 2021. Ancient and modern anastomosing rivers: insights from sedimentological and geomorphological case studies of the Triassic, Neogene and Holocene of Poland. *Geological Quarterly* 65, 54.
- Kruszewski, Ł., 2013. Supergene sulphate minerals from the burning coal mining dumps in the Upper Silesian Coal Basin, South Poland. *International Journal of Coal Geology* 105, 91–109.
- Laureijs, C., Coogan, L.A. & Spence, J., 2021. Regionally variable timing and duration of celadonite formation in the Troodos lavas (Cyprus) from Rb-Sr age distributions. *Chemical Geology* 560, 119995.
- Maciaszek, P., Chomiak, L., Urbański, P. & Widera, M., 2020. New insights into the genesis of the 'Poznań Clays' - upper Neogene of Poland. *Civil and Environmental Engineering Reports* 30, 18–32.
- McBride, E.F., 1974. Significance of color in red, green, purple, olive, brown, and gray beds of Difunta Group, northeastern Mexico. *Journal of Sedimentary Petrology* 44, 760–773.
- Mederski, S., Kruszewski, Ł. & Pršek, J., 2021. Epithermal Cu mineralization in the Stary Lesieniec rhyodacite quarry, Lower Silesia: primary and secondary mineral paragenesis. *Geological Quarterly* 65, 43.
- Murad, E., 2010. Mössbauer spectroscopy of clays, soils and their mineral constituents. *Clay Minerals* 45, 413–430.
- Murad, E. & Cashion, J., 2004. *Mössbauer spectroscopy of environmental materials and their industrial utilization*. Kluwer Academic Publishers, Norwell, Massachusetts, 417 pp.
- Myrow, M.M., 1990. A new graph for understanding colors of mudrocks and shales. *Journal of Geological Education* 38, 16–20.
- Piwocki, M. & Ziemińska-Tworzydło, M., 1997. Neogene of the Polish Lowlands - lithostratigraphy and pollen-spore zones. *Geological Quarterly* 41, 21–40.
- Piwocki, M., Badura, J. & Przybylski, B., 2004. Neogen. W: Peryt T.M., Piwocki M. (red.). *Budowa geologiczna Polski, t. 1, Stratygrafia część 3a, Kenozoik - paleogen, neogen* (in Polish): 71–133. Polish Geological Institute, Warszawa.
- Różycki, Z.R., 1972. *Plejstocen Polski Środkowej na tle przeszłości w górnym trzeciorzędzie* [The Pleistocene of central Poland against the background of the past in the upper Ter-

- tiary]. Państwowe Wydawnictwa Naukowe, Warszawa, 314 pp.
- Stevens, J.G., Khansanov, A.M., Miller, J.W., Pollak, H. & Li, Z., 2005. *Mössbauer Mineral Handbook. Mössbauer Effect Data Center, 3rd edition*. The University of North Carolina: Asheville, NC, USA, 636 pp.
- Tobia, F.H., Kettanah, Y.A. & Mustafa, M.M., 2014. Petrography and geochemistry of Ga'ara sedimentary ironstones, Western Desert of Iraq. *Journal of African Earth Sciences* 97, 261–272.
- Troć, M. & Sadowska, A., 2006. Wiek utworów formacji poznańskiej rejonu Poznania [The age of Poznań Formation in the area of Poznań]. *Przegląd Geologiczny* 54, 588–593.
- Tucker, M.E., 2011. *Sedimentary Rocks in the Field: A Practical Guide*. Wiley-Blackwell, Chichester, 304 pp.
- Valanciene, V., Siauciunas, R. & Baltusnikaite, J., 2010. The influence of mineralogical composition on the colour of clay body. *Journal of the European Ceramic Society* 30, 1609–1617.
- Wagner, M., 1982. Lithological-petrographical variability and depositional setting of the youngest Tertiary sediments in the Middle-Odra Trough. *Geologica Sudetica* 17, 57–101.
- Wichrowski, Z., 1981. Badania mineralogiczne ilów serii poznańskiej [Mineralogical studies of clays of the Poznań series]. *Archiwum Mineralogiczne* 37, 93–196.
- Widera, M., 2007. *Litostratygrafia i paleotektonika kenozoiku podplejstocenijskiego Wielkopolski [Lithostratigraphy and Palaeotectonics of the sub-Pleistocene Cenozoic of Wielkopolska]*. Adam Mickiewicz University Press, Poznań, 224 pp.
- Widera, M., 2013. Sand- and mud-filled fluvial palaeochannels in the Wielkopolska Member of the Neogene Poznań Formation, central Poland. *Annales Societatis Geologorum Poloniae* 83, 19–28.
- Widera, M., Chomiak, L. & Zieliński, T., 2019. Sedimentary facies, processes and paleochannel pattern of an anastomosing river system: an example from the Upper Neogene of Central Poland. *Journal of Sedimentary Research* 89, 487–507.
- Widera, M., Kowalska, E. & Fortuna, M., 2017. A Miocene anastomosing river system in the area of Konin Lignite Mine, central Poland. *Annales Societatis Geologorum Poloniae* 87, 157–168.
- Widera, M., Zieliński, T., Chomiak, L., Maciaszek, P., Wachocki, R., Bechtel, A., Słodkowska, B., Worobiec, E. & Worobiec, G., 2021. Tectonic-climatic interactions during changes of depositional environments in the Carpathian foreland: An example from the Neogene of central Poland. *Acta Geologica Polonica* 71, 519–542.
- Wiewióra, A. & Wyrwicki, R., 1976. Beidellite from the sediments of the Poznań series. *Kwartalnik Geologiczny* 20, 331–341.
- Wyrwicki, R. & Maliszewska, A., 1977. Utwory węglanowe w osadach ilastych serii poznańskiej (neogen). *Biuletyn Instytutu Geologicznego* 298, 269–314.
- Wyrwicki, R. & Wiewióra, A., 1981. Clay minerals of the Upper Miocene sediments in Poland. *Bulletin Polish Academy of Science, Earth Sciences* 29, 67–71.
- Zieliński, T. & Widera, M., 2020. Anastomosing-to-meandering transitional river in sedimentary record: A case study from the Neogene of central Poland. *Sedimentary Geology* 404, 105677.

Manuscript submitted: 23 March 2022

Revision accepted: 19 July 2022